

# IMPLEMENTATION OF GROUND INPUT MOTION AND DYNAMIC SOIL-STRUCTURE INTERACTION INTO OPENFAST FOR THE SEISMIC ANALYSIS OF OFFSHORE WIND TURBINES

Carlos Romero-Sánchez\* and Luis A. Padrón

Instituto Universitario de Sistemas Inteligentes y Aplicaciones Numéricas en Ingeniería  
Universidad de Las Palmas de Gran Canaria  
Las Palmas de Gran Canaria 35017, Spain  
e-mail: {carlos.romero, luis.padron}@ulpgc.es, web: <http://www.mmc.siani.es/>

**Keywords:** Offshore wind turbines, Soil-structure interaction, Seismic response, Lumped parameter models, OpenFAST

**Abstract.** *The development of offshore wind energy is expected to contribute significantly to the decarbonization of the electrical energy production sector, and the number of offshore wind farms is growing fast due to the maturity of the technology, the reduction in costs, and the increase in size and power of the turbines. Floating offshore wind is developing fast, but offshore wind turbines (OWTs) founded to the sea floor are still the dominant technology, with different types of support structures (monopiles, jackets, tripods) depending on the sea depth and the conditions of the location. The dynamic properties of these support structures are a key factor in the design of the system from a civil engineering point of view, and the distinctive features of OWTs (including the nature of the loads and the variable geometry of the system due to the rotation of the blades and the continuous actions of the control system) suggest that specific tools, able to adequately model the different subsystems, should be used in structural and seismic analyses. For this reason, input ground motion and dynamic soil-structure interaction capabilities have been implemented in OpenFAST, an open-source nonlinear aero-hydro-servo-elastic code for the simulation of wind turbines, in which the environmental loads and the response of all the main elements are taken into account through specific models and modules. This paper presents the equations of motion and the specific procedure followed to implement input ground motion and soil-structure interaction into the SubDyn module, and presents validation results to illustrate the applicability of the approach.*

## 1 INTRODUCTION

Geopolitical instabilities and military tensions with Russia, added to the current Climate Emergency situation, show once again that Europe needs to move fast towards energy independence based on renewable energies with the lowest possible environmental impact. Among the renewable energy sources of these characteristics available in Europe, and in which Europe can be independent to a large extent, we can mention offshore wind energy, whose potential is much greater than of onshore energy. Most of the offshore wind turbines installed in Europe are located in places where the depth of the sea allows founding them directly to the seabed. Floating wind turbines is growing in the last years, however, in Europe monopiles remain the preferred choice of developers, 80.5% new installation in 2020 and 19% on jackets [1].

With the expansion in the number of wind farms comes the need of placing new offshore wind turbines in locations with worse geotechnical properties, greater depths and increasing seismic risk. Therefore, there exists the need for numerical tools to study the seismic response of offshore wind turbines, regardless of their structural typology, and including the phenomena of soil-structure interaction and kinematic interaction between foundations and incident seismic waves. There are many models with different levels of simplification to do this for offshore wind turbines, but it is ideal to have an advanced tool that can take into account the different subsystems that composed a wind turbine. In this regard, an interesting option is OpenFAST [2], which is a multi-physics, multi-fidelity tool for simulating the coupled dynamic response of wind turbines. It is open-source, is programmed in Fortran 95, and it might be considered not as a single program, but as a framework that couples computational modules for aerodynamics, hydrodynamics for offshore structures, control and electrical system (servo) dynamics, and structural dynamics to enable coupled nonlinear aero-hydro-servo-elastic simulation in the time domain. The main modules regarding the dynamic response of the system are: BeamDyn for modelling the dynamic behaviour of the blades; ServoDyn for modelling the generator and the control system; ElastoDyn for modelling the dynamic response of the tower in the fore-aft and side-to-side directions, and based on a modal approach that takes into account only the first two vibration modes in each direction; and SubDyn for modelling the dynamic response of the substructure, from the Transition Piece (TP) at the base of the structure to the base. In this work, the proposed modifications will be implemented in this last module, SubDyn. The different modules interact in a loosely coupled time-integration scheme, where a glue-code transfers data among modules at each time step. This glue code is the FAST driver, that gathers all the information and drives the time-domain solution forward step-by-step using a predictor-corrector scheme. Each module inputs and outputs relevant information. For more information, OpenFAST documentation [2]. Thus, this paper presents the implementation of seismic input motions and dynamic soil-structure interaction into OpenFAST. The first item includes not only horizontal ground input motions, but translational, vertical and rotational foundation input motions, while the second aspect is introduced through a simplified lumped parameter model that is

previously fitted to represent the dynamic response of the foundation. The use of lumped parameter models is considered here as a tool to introduce dynamic soil-structure interaction into the model because, contrary to a static stiffness matrix, this approach allows to take into account, not only the static stiffness of the foundation, but an approximation to its impedance, i.e., the dynamic stiffness and damping functions. This damping, arising not only from material damping but most importantly from radiation damping, can be relevant in the dynamic response of the structure. These capabilities have been implemented in OpenFAST, version 2.2.0, and the code can be downloaded here: [https://github.com/CarlosRomeroSanchez/openfast.2.2.0\\_seismic](https://github.com/CarlosRomeroSanchez/openfast.2.2.0_seismic) .

This paper presents, firstly, a general overview of the original formulation implemented in the SubDyn module. Then, the proposed formulation is presented and verified by comparison against a different simplified model for some specific verification cases. Finally, results of a specific illustration example are presented.

## 2 GENERAL OVERVIEW OF THE FINITE ELEMENTS METHOD FORMULATION IMPLEMENTED IN SUBDYN.

This section presents a general overview of SubDyn [3]. The module integrates its equations through its own solver. The main steps are: discretization of the substructuring following the strategies of classical linear beam Finite Elements motion equations, application of Craig-Bampton modal reduction and rearrangement of the equations into State-Space type formulation for time-domain resolution and coupling with the rest of modules.

### 2.1 Dynamic System of Equations

The structure is discretized with the following simplifying assumptions: Two-noded Euler-Bernoulli or Timoshenko three-dimensional beams with 12 degrees of freedom, linear response and rigid joints, leading to a classical equation of motion of the type:

$$\mathbf{M}\ddot{u}(t) + \mathbf{C}\dot{u}(t) + \mathbf{K}u(t) = F(t) \quad (1)$$

$$\begin{bmatrix} M_{RR} & M_{RL} \\ M_{LR} & M_{LL} \end{bmatrix} \begin{pmatrix} \ddot{u}_R \\ \ddot{u}_L \end{pmatrix} + \begin{bmatrix} C_{RR} & C_{RL} \\ C_{LR} & C_{LL} \end{bmatrix} \begin{pmatrix} \dot{u}_R \\ \dot{u}_L \end{pmatrix} + \begin{bmatrix} K_{RR} & K_{RL} \\ K_{LR} & K_{LL} \end{bmatrix} \begin{pmatrix} u_R \\ u_L \end{pmatrix} = \begin{pmatrix} F_R \\ F_L \end{pmatrix} \quad (2)$$

where  $M$ ,  $C$  and  $K$  are the global mass, damping and stiffness matrices,  $u$  and  $F$  are the displacements and external forces along all of the DOFs of the assembled system. The subindex R identifies the boundary nodes (at the base and at the Transition Piece) and L identifies the rest of nodes (interior nodes).

### 2.2 Craig-Bampton modal reduction

The Craig-Bampton method reduces the number of the internal generalized degrees of freedom of the substructure, using a subset  $q_m$  ( $m \leq L$ ). Equation (3) relates physical

DOFs and generalized DOFs ( $q_L$ ):

$$\begin{Bmatrix} U_R \\ U_L \end{Bmatrix} = \begin{bmatrix} I & 0 \\ \Phi_R & \Phi_L \end{bmatrix} \begin{Bmatrix} U_R \\ q_L \end{Bmatrix} \quad (3)$$

where  $I$  is the identity matrix;  $\Phi_R$  (matrix) represents the physical displacements of the interior nodes for static, rigid body motion at the boundary and  $\Phi_L$  (matrix) represents the internal eigenmodes. The Craig-Bampton transformation is therefore represented by:

$$\begin{Bmatrix} U_R \\ U_L \end{Bmatrix} = \begin{bmatrix} I & 0 \\ \Phi_R & \Phi_m \end{bmatrix} \begin{Bmatrix} U_R \\ q_m \end{Bmatrix} \quad (4)$$

where  $\Phi_m$  is the matrix that represents the truncated set of  $\Phi_L$ . Premultiplying both sides by equation (2) yields:

$$\begin{bmatrix} M_{BB} & M_{Bm} \\ M_{mB} & I \end{bmatrix} \begin{pmatrix} \ddot{u}_R \\ \ddot{q}_m \end{pmatrix} + \begin{bmatrix} C_{BB} & C_{Bm} \\ C_{mB} & 2\zeta\Omega_m \end{bmatrix} \begin{pmatrix} \dot{u}_R \\ \dot{q}_m \end{pmatrix} + \begin{bmatrix} K_{BB} & 0 \\ 0 & \Omega_m^2 \end{bmatrix} \begin{pmatrix} u_R \\ q_m \end{pmatrix} = \begin{pmatrix} F_B \\ F_m \end{pmatrix} \quad (5)$$

where:

$$M_{BB} = M_{RR} + M_{RL}\Phi_R + \Phi_R^T M_{LR} + \Phi_R^T M_{LL}\Phi_R \quad (6)$$

$$C_{BB} = C_{RR} + C_{RL}\Phi_R + \Phi_R^T C_{LR} + \Phi_R^T C_{LL}\Phi_R \quad (7)$$

$$K_{BB} = K_{RR} + K_{RL}\Phi_R \quad (8)$$

$$M_{mB} = \Phi_m^T M_{LR} + \Phi_m^T M_{LL}\Phi_R \quad (9)$$

$$C_{mB} = \Phi_m^T C_{LR} + \Phi_m^T C_{LL}\Phi_R \quad (10)$$

$$M_{Bm} = M_{mB}^T, C_{Bm} = C_{mB}^T \quad (11)$$

$$F_B = F_R + \Phi_R^T F_L \quad (12)$$

$$F_M = \Phi_M^T F_L \quad (13)$$

After modal decomposition, this superposition is made not with all modes, but with only a few ( $m$  modes), as usual in this kind of strategies, leading to a significant decrease in the number of degrees of freedom of the system. Introducing this idea into the FEM equations, and concentrating the motions at the boundary in the Transition Piece of the OWT (joint between tower and substructure) the equations are written as:

$$\begin{bmatrix} \tilde{M}_{BB} & \tilde{M}_{Bm} \\ \tilde{M}_{mB} & I \end{bmatrix} \begin{pmatrix} \ddot{u}_{tp} \\ \ddot{q}_m \end{pmatrix} + \begin{bmatrix} \tilde{C}_{BB} & \tilde{C}_{Bm} \\ \tilde{C}_{mB} & 2\zeta\Omega_m \end{bmatrix} \begin{pmatrix} \dot{u}_{tp} \\ \dot{q}_m \end{pmatrix} + \begin{bmatrix} \tilde{K}_{BB} & 0 \\ 0 & \Omega_m^2 \end{bmatrix} \begin{pmatrix} u_{tp} \\ q_m \end{pmatrix} = \begin{pmatrix} \tilde{F}_{tp} \\ \tilde{F}_m \end{pmatrix} \quad (14)$$

where the overhead bar here and below denotes matrices/vectors after the fixed-bottom boundary conditions are applied.  $u_{tp}$  is the 6 DOFs of the rigid transition piece.

### 2.3 State-space formulation

To arrange variables in sets of inputs and outputs that can communicate with the rest of modules, the equations are cast in state-space formulation, defining  $x = x(t) = (q_m \quad \dot{q}_m)^T$  as the states;  $u = (U_{TP} \quad \dot{U}_{TP} \quad \ddot{U}_{TP} \quad F_{L,e} \quad F_{R,e})^T$  as the inputs from other modules;  $Y_1 = Y_1(t) = -F_{TP}$  as outputs to tower (ElastoDyn);  $Y_2 = Y_2(t)$  as outputs to HydroDyn (motion of the substructure).

Then, equation 14 can be cast into state equation form as:

$$\dot{x} = Ax + Bu + F_x \quad (15)$$

$$-Y_1 = C_1x + D_1u + F_{y1} \quad (16)$$

$$Y_2 = C_2x + D_2u + F_{y2} \quad (17)$$

where  $A, B, F_x, C_1, C_2, D_1, D_2, F_{y1}$  and  $F_{y2}$  are arrays and matrices of constant coefficients that are computed only, at initialization.

## 3 IMPLEMENTATION OF UNIFORM BASE INPUT MOTION AND SOIL-STRUCTURE INTERACTION MODEL INTO SUBDYN MODULE

### 3.1 Generic equation of motion

Equation (1) assumes fixed-base, taking into account prescribed displacement in the base, the main equations of motion describing the dynamic response of the substructure can be written as:

$$\mathbf{M}\ddot{u}^t(t) + \mathbf{C}\dot{u}^t(t) + \mathbf{K}u^t(t) = F(t) \quad (18)$$

where now  $u$  and  $u^t$  represent relative and total displacements. If kinematic input motion at time  $t$ , taking into account the presence of the foundation and its interaction with the incident seismic field, is denoted by vector  $u_b(t)$  ( $u_b = U, V, \theta$ ), the relationship between displacements can be written as:

$$u(t) = u^t(t) - \Lambda u_b(t) \quad (19)$$

where  $\Lambda$  is a matrix composed by  $\Lambda_U, \Lambda_V$  and  $\Lambda_\theta$ , which the influence vectors (Chopra [4]) representing the displacement of the different degrees of freedom as a consequence of the static application of unitary lateral, vertical or rotational ground displacements, respectively. Writing the equation of motion in absolute terms yield:

$$\mathbf{M}\ddot{u}^t(t) + \mathbf{C}\dot{u}^t(t) + \mathbf{K}u^t(t) = F(t) + \mathbf{C}\Lambda\dot{u}_b(t) + \mathbf{K}\Lambda u_b(t) \quad (20)$$

After the assembly, the system of equation can be written as:

$$\begin{bmatrix} M_{RR} & M_{RL} \\ M_{LR} & M_{LL} \end{bmatrix} \begin{pmatrix} \ddot{u}_R \\ \ddot{u}_L \end{pmatrix}^t + \begin{bmatrix} C_{RR} & C_{RL} \\ C_{LR} & C_{LL} \end{bmatrix} \begin{pmatrix} \dot{u}_R \\ \dot{u}_L \end{pmatrix}^t + \begin{bmatrix} K_{RR} & K_{RL} \\ K_{LR} & K_{LL} \end{bmatrix} \begin{pmatrix} u_R \\ u_L \end{pmatrix}^t = \begin{pmatrix} F_R \\ F_L \end{pmatrix} + \begin{bmatrix} C_{RR} & C_{RL} \\ C_{LR} & C_{LL} \end{bmatrix} \begin{pmatrix} \Lambda_R \\ \Lambda_L \end{pmatrix} \dot{u}_b + \begin{bmatrix} K_{RR} & K_{RL} \\ K_{LR} & K_{LL} \end{bmatrix} \begin{pmatrix} \Lambda_R \\ \Lambda_L \end{pmatrix} u_b \quad (21)$$

where  $F_R = F_{R,e} + F_{R,g}$ , with  $F_{R,e}$  being external loads from other modules, the hydrodynamic forces over the boundary nodes and the forces transferred to and from ElastoDyn through the Transition Piece; and  $g$  stands for the gravity loads.

The interior degrees of freedom are hence transformed from physical DOFs to modal DOFs, and pre-multiplying by Craig-Bampton transformation (equation 4) both sides of equation of motion, can be rewritten as:

$$\begin{aligned} \begin{bmatrix} M_{BB} & M_{Bm} \\ M_{mB} & I \end{bmatrix} \begin{pmatrix} \ddot{u}_R \\ \ddot{q}_m \end{pmatrix}^t + \begin{bmatrix} C_{BBf} & C_{Bm_f} \\ C_{mB_f} & C_{mm_f} + 2\zeta\Omega_m \end{bmatrix} \begin{pmatrix} \dot{u}_R \\ \dot{q}_m \end{pmatrix}^t + \begin{bmatrix} K_{BB} & 0 \\ 0 & \Omega_m^2 \end{bmatrix} \begin{pmatrix} u_R \\ q_m \end{pmatrix}^t = \\ \begin{pmatrix} F_R + \Phi_R^T F_L \\ \Phi_m^T F_L \end{pmatrix} + \begin{bmatrix} C_{BBf} & C_{Bm_f} \\ C_{mB_f} & C_{mm_f} + 2\zeta\Omega_m \end{bmatrix} \begin{pmatrix} \Lambda_R \\ \Lambda_m \end{pmatrix} \dot{u}_b + \begin{bmatrix} K_{BB} & 0 \\ 0 & \Omega_m^2 \end{bmatrix} \begin{pmatrix} \Lambda_R \\ \Lambda_m \end{pmatrix} u_b \end{aligned} \quad (22)$$

where the damping matrix is composed of the structural damping ( $2\zeta\Omega_m$ ) and damping terms related to the LPM foundation model ( $C_f$ ). On the other hand,  $\Lambda_m$  is obtained as the truncation of  $\Lambda_L$  as:

$$\Lambda_L = \Phi_R \Lambda_R + \Phi_m \Lambda_M \quad (23)$$

$$\Lambda_m = \bar{\Lambda}_L \quad (24)$$

### 3.2 Equation of motion with lateral, vertical and rotational foundation input motion

The vector of displacements at the boundary nodes contains the displacement at the interface node with the tower ( $u_I$ ) and the displacements at base nodes, which would move following the ground motion according to the relevant portion  $\Lambda$  of the influence vector:

$$u_R = \begin{pmatrix} \Lambda_U U_b + \Lambda_\theta \theta_b + \Lambda_V V_b \\ u_I \end{pmatrix} \quad (25)$$

where  $U_b$  is the lateral kinematic input motion,  $V_b$  is the vertical kinematic input motion and  $\theta_b$  is the rotational kinematic input motion. Accordingly, the matrices of related to the boundary nodes can be decompose as:

$$M_{BB} = \begin{bmatrix} M_{bb} & M_{bI} \\ M_{Ib} & \bar{M}_{BB} \end{bmatrix} ; \quad M_{Bm} = \begin{bmatrix} M_{bm} \\ \bar{M}_{Bm} \end{bmatrix} ; \quad M_{mB} = \begin{bmatrix} M_{mb} \\ \bar{M}_{mB} \end{bmatrix} \quad (26)$$

where  $b$  is base nodes and  $I$  is interface nodes. The overhead bar here and below denotes matrices/vectors after the fixed-bottom boundary condition are applied.

$$\begin{aligned}
 \begin{bmatrix} \bar{M}_{BB} & \bar{M}_{Bm} \\ \bar{M}_{mB} & I \end{bmatrix} \begin{pmatrix} \ddot{u}_{tp} \\ \ddot{q}_m \end{pmatrix}^t + \begin{bmatrix} \bar{C}_{BBf} & \bar{C}_{Bm_f} \\ \bar{C}_{mB_f} & C_{mm_f} + 2\zeta\Omega_m \end{bmatrix} \begin{pmatrix} \dot{u}_{tp} \\ \dot{q}_m \end{pmatrix}^t + \begin{bmatrix} \bar{K}_{BB} & 0 \\ 0 & \Omega_m^2 \end{bmatrix} \begin{pmatrix} u_{tp} \\ q_m \end{pmatrix}^t = \\
 \begin{pmatrix} \bar{F}_R + \Phi_R^T F_L \\ \Phi_m^T F_L \end{pmatrix} + \begin{bmatrix} \bar{C}_{BBf} & \bar{C}_{Bm_f} \\ \bar{C}_{mB_f} & C_{MM} + 2\zeta\Omega_m \end{bmatrix} \begin{pmatrix} \Lambda_I \\ \Lambda_m \end{pmatrix} \dot{u}_b + \\
 \begin{bmatrix} \bar{K}_{BB} & 0 \\ 0 & \Omega_m^2 \end{bmatrix} \begin{pmatrix} \Lambda_I \\ \Lambda_m \end{pmatrix} u_b - \begin{bmatrix} M_{Ib} \\ M_{mb} \end{bmatrix} \Lambda_b \ddot{u}_b \quad (27)
 \end{aligned}$$

The interfaces nodes and the Transition Piece (that is assumed as a rigid body) are considered as rigidly connected, so that the following relationships hold:

$$u_I = T_I u_{tp} \quad (28)$$

$$F_{tp} = T_I^T F_R \quad (29)$$

where  $T_I$  is a simple transformation matrix depending on the differences between the locations between both points. Taking these two relations into account, eq. (27) can be written as:

$$\begin{aligned}
 \begin{bmatrix} \tilde{M}_{BB} & \tilde{M}_{Bm} \\ \tilde{M}_{mB} & I \end{bmatrix} \begin{pmatrix} \ddot{u}_{tp} \\ \ddot{q}_m \end{pmatrix}^t + \begin{bmatrix} \tilde{C}_{BBf} & \tilde{C}_{Bm_f} \\ \tilde{C}_{mB} & C_{mm} + 2\zeta\Omega_m \end{bmatrix} \begin{pmatrix} \dot{u}_{tp} \\ \dot{q}_m \end{pmatrix}^t + \begin{bmatrix} \tilde{K}_{BB} & 0 \\ 0 & \Omega_m^2 \end{bmatrix} \begin{pmatrix} u_{tp} \\ q_m \end{pmatrix}^t = \\
 \begin{pmatrix} \tilde{F}_{tp} \\ \tilde{F}_m \end{pmatrix} + \begin{bmatrix} F_{I\text{sis}K-U} \\ F_{M\text{sis}K-U} \end{bmatrix} U_b(t) + \begin{bmatrix} F_{I\text{sis}C-U} \\ F_{M\text{sis}C-U} \end{bmatrix} \dot{U}_b(t) - \begin{bmatrix} F_{I\text{sis}M-U} \\ F_{M\text{sis}M-U} \end{bmatrix} \ddot{U}_b(t) \\
 + \begin{bmatrix} F_{I\text{sis}K-V} \\ F_{M\text{sis}K-V} \end{bmatrix} V_b(t) + \begin{bmatrix} F_{I\text{sis}C-V} \\ F_{M\text{sis}C-V} \end{bmatrix} \dot{V}_b(t) - \begin{bmatrix} F_{I\text{sis}M-V} \\ F_{M\text{sis}M-V} \end{bmatrix} \ddot{V}_b(t) \\
 + \begin{bmatrix} F_{I\text{sis}K-\theta} \\ F_{M\text{sis}K-\theta} \end{bmatrix} \theta_b(t) + \begin{bmatrix} F_{I\text{sis}C-\theta} \\ F_{M\text{sis}C-\theta} \end{bmatrix} \dot{\theta}_b(t) - \begin{bmatrix} F_{I\text{sis}M-\theta} \\ F_{M\text{sis}M-\theta} \end{bmatrix} \ddot{\theta}_b(t) \quad (30)
 \end{aligned}$$

where:

$$\tilde{M}_{BB} = T_I^T \bar{M}_{BB} T_I \quad (31)$$

$$\tilde{C}_{BBf} = T_I^T \bar{C}_{BBf} T_I \quad (32)$$

$$\tilde{K}_{BB} = T_I^T \bar{K}_{BB} T_I \quad (33)$$

$$\tilde{M}_{Bm} = T_I^T \bar{M}_{Bm} \quad (34)$$

$$\tilde{C}_{Bm_f} = T_I^T \bar{C}_{Bm_f} \quad (35)$$

$$\tilde{F}_{tp} = F_{tp} + T_I^T \bar{F}_{R,e} + T_I^T \bar{F}_{R,g} + T_I^T \bar{\Phi}_R^T (F_{L,e} + F_{L,g}) \quad (36)$$

$$\tilde{F}_m = \Phi_m^T (F_{L,e} + F_{L,g}) \quad (37)$$

$$F_{I\text{sis}K-U} = T_I^T (\bar{K}_{BB} \Lambda_{U_I}) \quad (38)$$

$$F_{M\text{sis}K-U} = \Omega_m^2 \Lambda_{U_m} \quad (39)$$

$$F_{I\text{sis}C-U} = T_I^T (\bar{C}_{BB_f} \Lambda_{U_I} + \bar{C}_{Bm_f} \Lambda_{U_m}) \quad (40)$$

$$F_{M\text{sis}C-U} = \bar{C}_{mB_f} \Lambda_{U_I} + (C_{mm_f} + 2\zeta\Omega_m) \Lambda_{U_m} \quad (41)$$

$$F_{I\text{sis}M-U} = T_I^T \bar{M}_{Ib} \Lambda_{U_b} \quad (42)$$

$$F_{M\text{sis}M-U} = M_{Mb} \Lambda_{U_b} \quad (43)$$

$$F_{I\text{sis}K-\theta} = T_I^T (\bar{K}_{BB} \Lambda_{\theta_I}) \quad (44)$$

$$F_{M\text{sis}K-\theta} = \Omega_m^2 \Lambda_{\theta_m} \quad (45)$$

$$F_{I\text{sis}C-\theta} = T_I^T (\bar{C}_{BB_f} \Lambda_{\theta_I} + \bar{C}_{Bm_f} \Lambda_{\theta_m}) \quad (46)$$

$$F_{M\text{sis}C-\theta} = \bar{C}_{mB_f} \Lambda_{\theta_I} + (C_{mm_f} + 2\zeta\Omega_m) \Lambda_{\theta_m} \quad (47)$$

$$F_{I\text{sis}M-\theta} = T_I^T \bar{M}_{Ib} \Lambda_{\theta_b} \quad (48)$$

$$F_{M\text{sis}M-\theta} = M_{Mb} \Lambda_{\theta_b} \quad (49)$$

$$F_{I\text{sis}K-V} = T_I^T (\bar{K}_{BB} \Lambda_{V_I}) \quad (50)$$

$$F_{M\text{sis}K-V} = \Omega_m^2 \Lambda_{V_m} \quad (51)$$

$$F_{I\text{sis}C-V} = T_I^T (\bar{C}_{BB_f} \Lambda_{V_I} + \bar{C}_{Bm_f} \Lambda_{V_m}) \quad (52)$$

$$F_{M\text{sis}C-V} = \bar{C}_{mB_f} \Lambda_{V_I} + (C_{mm_f} + 2\zeta\Omega_m) \Lambda_{V_m} \quad (53)$$

$$F_{I\text{sis}M-V} = T_I^T \bar{M}_{Ib} \Lambda_{V_b} \quad (54)$$

$$F_{M\text{sis}M-V} = M_{Mb} \Lambda_{V_b} \quad (55)$$

### 3.3 Simplified Lumped Model Parameter Model into SubDyn

The introduction of an LPM can be simply understood as adding one (or several) additional elements at the base of the substructure. At this point, the simplified Lumped Parameter Model proposed by Carbonari et al. [5], depicted in figure 1, is adopted for the lateral vibrations, while the spring-damper model depicted in figure 2 is adopted for vertical and torsional vibrations (assuming that their influence on the response of the system is, in any case, smaller). These assumptions lead to the following stiffness, damping and mass matrices:

$$\mathbf{K} = \begin{bmatrix} \mathbf{K}_{ii} & \mathbf{K}_{ij} \\ (\text{sym}) & \mathbf{K}_{jj} \end{bmatrix}; \quad \mathbf{C} = \begin{bmatrix} \mathbf{C}_{ii} & \mathbf{C}_{ij} \\ (\text{sym}) & \mathbf{C}_{jj} \end{bmatrix}; \quad \mathbf{M} = \begin{bmatrix} \mathbf{0} & \mathbf{0} \\ (\text{sym}) & \mathbf{M}_{jj} \end{bmatrix} \quad (56)$$

where node  $i$  is the ground, node  $j$  is the base of the substructure, and the submatrices are defined as follows:

$$u_b^T = [ u_{xb} \quad u_{yb} \quad u_{zb} \quad \theta_{xb} \quad \theta_{yb} \quad \theta_{zb} ] \quad (57)$$

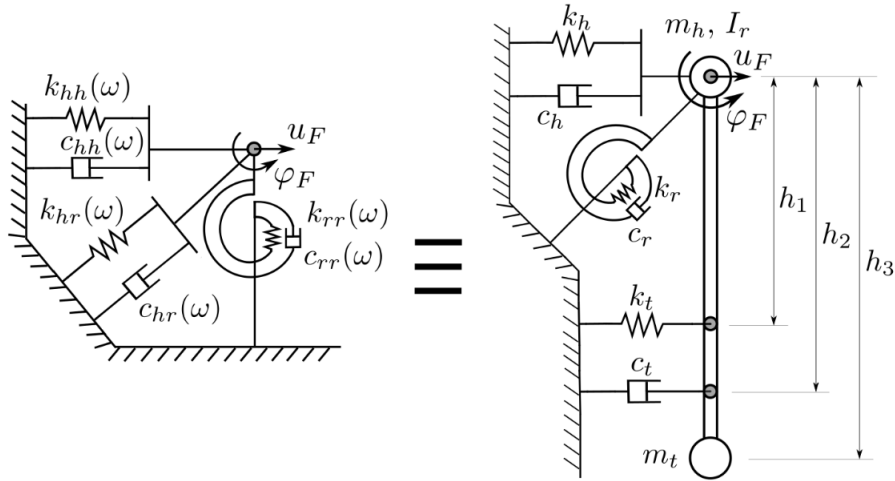


Figure 1. Scheme of the simplified LPM, adopted for lateral vibrations [6]

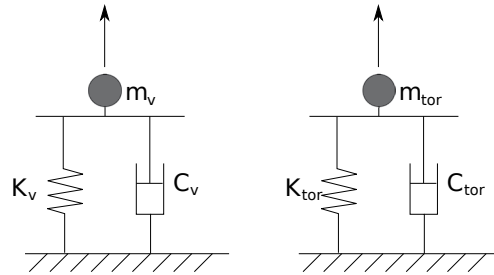


Figure 2. Scheme of the mass-spring-damper model, adopted for vertical and torsional vibrations [6]

$$\mathbf{K}_{jj} = \begin{bmatrix} k_h + k_t & 0 & 0 & 0 & -k_t h_1 & 0 \\ & k_h + k_t & 0 & k_t h_1 & 0 & 0 \\ & & k_z & 0 & 0 & 0 \\ & & & k_r + k_t h_1^2 & 0 & 0 \\ & & & & k_r + k_t h_1^2 & 0 \\ & & & & & k_{tor} \end{bmatrix} \quad (58)$$

$$\mathbf{K}_{ji} = \mathbf{K}_{ij}^T = \begin{bmatrix} -(k_h + k_t) & 0 & 0 & 0 & k_t h_1 & 0 \\ 0 & -(k_h + k_t) & 0 & -k_t h_1 & 0 & 0 \\ 0 & 0 & -k_z & 0 & 0 & 0 \\ 0 & k_t h_1 & 0 & -(k_r + k_t h_1^2) & 0 & 0 \\ -k_t h_1 & 0 & 0 & 0 & -(k_r + k_t h_1^2) & 0 \\ 0 & 0 & 0 & 0 & 0 & -k_{tor} \end{bmatrix} \quad (59)$$

$$\mathbf{C}_{jj} = \begin{bmatrix} c_h + c_t & 0 & 0 & 0 & -c_t h_2 & 0 \\ & c_h + c_t & 0 & c_t h_2 & 0 & 0 \\ & & c_z & 0 & 0 & 0 \\ & & & c_r + c_t h_2^2 & 0 & 0 \\ & & & & c_r + c_t h_2^2 & 0 \\ & & & & & c_{\text{tor}} \end{bmatrix} \quad (60)$$

$$\mathbf{C}_{ji} = \mathbf{C}_{ij}^T = \begin{bmatrix} -(c_h + c_t) & 0 & 0 & 0 & c_t h_2 & 0 \\ 0 & -(c_h + c_t) & 0 & -c_t h_2 & 0 & 0 \\ 0 & 0 & -c_z & 0 & 0 & 0 \\ 0 & c_t h_2 & 0 & -(c_r + c_t h_2^2) & 0 & 0 \\ -c_t h_2 & 0 & 0 & 0 & -(c_r + c_t h_2^2) & 0 \\ 0 & 0 & 0 & 0 & 0 & -c_{\text{tor}} \end{bmatrix} \quad (61)$$

$$\mathbf{M}_{jj} = \begin{bmatrix} m_h + m_t & 0 & 0 & 0 & -m_t h_3 & 0 \\ & m_h + m_t & 0 & m_t h_3 & 0 & 0 \\ & & m_z & 0 & 0 & 0 \\ & & & I_r + m_t h_3^2 & 0 & 0 \\ & & & & I_r + m_t h_3^2 & 0 \\ & & & & & I_{\text{tor}} \end{bmatrix} \quad (62)$$

where the SLPM coefficients are calculated using least squares to be optimally adapted to the impedance functions defining the dynamic response of the wind turbine foundation.

### 3.4 State-space formulation

These equations must be cast in a form useful for implementation into the general framework of OpenFAST and SubDyn, taking into account which are the input variables to SubDyn and the output variables from SubDyn to other modules. The equations are written in state-space form. The states are defined as:

$$x = \left( q_m^t \quad \dot{q}_m^t \right)^T \quad (63)$$

and the input vector are defined as:

$$u = \left( U_{tp}^t \quad \dot{U}_{tp}^t \quad \ddot{U}_{tp}^t \quad F_{L,e} \quad F_{R,e} \right)^T \quad (64)$$

#### 3.4.1 State equation

Equation (30) is cast into standard linear system state equation of the form:

$$\dot{x} = X = \mathbf{A}x + \mathbf{B}u + F_x \quad (65)$$

To do, the second row of equation (30) needs to be written down and solved for  $\ddot{U}_L$ . After doing so, the matrices of the state equation can be found to be:

$$\mathbf{A} = \begin{bmatrix} 0 & I \\ -\Omega_m^2 & -C_{mmf} - 2\zeta\Omega_m \end{bmatrix} \quad (66)$$

$$\mathbf{B} = \begin{bmatrix} 0 & 0 & 0 & 0 & 0 \\ 0 & -\tilde{C}_{mB_f} & -\tilde{M}_{mB} & \Phi_m^T & 0 \end{bmatrix} \quad (67)$$

$$Fx = \begin{bmatrix} 0 \\ \Phi_m^T F_{Lg} + \sum_i F_{MsisK-i} u_b + \sum_i F_{MsisC-i} \dot{u}_b - \sum_i F_{MsisM-i} \ddot{u}_b \end{bmatrix} \quad (68)$$

where I is the identity matrix and  $i = U, V, \theta$

### 3.4.2 Output equation to ElastoDyn

The first output equation computes the interaction forces between tower and substructure at the Transition Piece.

$$y_1 = Y_1 = -F_{tp} \quad (69)$$

Writting the first row of (30) and solving for  $F_{tp}$ , the output equation can be written as:

$$-Y_1 = \mathbf{C}_1 x + \mathbf{D}_1 \bar{u} + F_{y_1} \quad (70)$$

where

$$\mathbf{C}_1 = \begin{bmatrix} -\tilde{M}_{Bm}\Omega_m^2 & -\tilde{M}_{Bm}(C_{mmf} + 2\zeta\Omega_m) + \tilde{C}_{Bm} \end{bmatrix} \quad (71)$$

$$\mathbf{D}_1 = \begin{bmatrix} \tilde{K}_{BB} & -\tilde{C}_{mB_f}\tilde{M}_{Bm} + \tilde{C}_{BB_f} & -\tilde{M}_{mB}\tilde{M}_{Bm} + \tilde{M}_{BB} & \tilde{M}_{Bm}\Phi_m^T - T_I^T\Phi_R^T & -T_I^T \end{bmatrix} \quad (72)$$

$$F_{y_1} = -T_I^T(\bar{F}_{Ig} + \bar{\Phi}_R^T F_{Lg}) - \sum_i F_{IsisK-i} u_b - \sum_i F_{IsisC-i} \dot{u}_b + \sum_i F_{IsisM-i} \ddot{u}_b + \tilde{M}_{Bm} \left[ \sum_i F_{MsisK-i} u_b + \sum_i F_{MsisC-i} \dot{u}_b - \sum_i F_{MsisM-i} \ddot{u}_b + \Phi_m^T F_{Lg} \right]; i = U, V, \theta \quad (73)$$

### 3.4.3 Output equation to HydroDyn

The second output equation gathers all the motions needed by the module HydroDyn to compute hydrodynamic loads on the substructure.

$$y_2 = Y_2 = \{ u_I^t \quad u_L^t \quad \dot{u}_I^t \quad \dot{u}_L^t \quad \ddot{u}_I^t \quad \ddot{u}_L^t \}^T \quad (74)$$

$$Y_2 = \mathbf{C}_2 x + \mathbf{D}_2 u + F_{y_2} \quad (75)$$

where

$$\mathbf{C}_2 = \begin{bmatrix} 0 & 0 \\ \Phi_m & 0 \\ 0 & 0 \\ 0 & \Phi_m \\ 0 & 0 \\ -\Phi_m \Omega_m^2 & -\Phi_m (C_{mmf} + 2\zeta \Omega_m) \end{bmatrix} \quad (76)$$

$$\mathbf{D}_2 = \begin{bmatrix} T_I & 0 & 0 & 0 & 0 \\ \bar{\Phi}_R T_I & 0 & 0 & 0 & 0 \\ 0 & T_I & 0 & 0 & 0 \\ 0 & \bar{\Phi}_R T_I & 0 & 0 & 0 \\ 0 & 0 & T_I & 0 & 0 \\ 0 & -\Phi_m \tilde{C}_{mBf} & \tilde{\Phi}_R T_I - \Phi_m \tilde{M}_{mB} & \Phi_m \Phi_m^T & 0 \end{bmatrix} \quad (77)$$

$$F_{y_2} = \begin{bmatrix} 0 \\ 0 \\ 0 \\ 0 \\ 0 \\ \Phi_m \Phi_m^T F_{Lg} + \Phi_m (\sum_i F_{MsisK-i} u_b + \sum_i F_{MsisC-i} \dot{u}_b - \sum_i F_{MsisM-i} \ddot{u}_b) \end{bmatrix} \quad (78)$$

where  $i = U, \theta, V$ .

## 4 VERIFICATION RESULTS

The correct implementation into OpenFAST of the input ground motion and the simplified Lumped Parameter Model at the base of the substructure has been initially verified by comparison against results obtained from a simplified model written in matlab for this purpose. Firstly, this model is first briefly described. Afterwards, the cases designed for verification are presented and the results of the comparison are shown.

### 4.1 Reference simple model for comparison

The model used for comparison is depicted in figure 3. It can be understood as an inverted pendulum on a beam comprised of two different parts: the inferior part corresponding to the substructure with constant properties along height; and the upper part corresponding to the tower, with varying properties along height. On top, the rotor-nacelle-assembly (RNA) is modeled as a punctual rigid concentrated inertia. The model can be run as fixed based or as compliant base.

Again, the equation of motion can be written as:

$$\mathbf{M} \ddot{u}^t(t) + \mathbf{C} \dot{u}^t(t) + \mathbf{K} u^t(t) = \mathbf{0} \quad (79)$$

where  $\mathbf{M}$ ,  $\mathbf{C}$  and  $\mathbf{K}$  are the mass, damping and stiffness matrices. The beam elements implemented are identical to those already implemented in SubDyn. Vectors  $u$  and  $u^t$  represent relative and total (or absolute) displacements at the different DOFs in the structure. If the input ground displacement at time  $t$  is denoted by  $u_b(t)$ , and eq. (19) is taken into account, the equation of motion in relative terms, yields:

$$\mathbf{M} \ddot{u}(t) + \mathbf{C} \dot{u}(t) + \mathbf{K} u(t) = -\mathbf{M}\Lambda \ddot{u}_b(t) \quad (80)$$

Assuming steady-state harmonic response, motions can be written as:

$$u(t) = U(\omega)e^{i\omega t} \quad (81)$$

where  $\omega$  is the circular frequency of the excitation. Thus, the time-harmonic equation of motion employed can be written as:

$$(\mathbf{K} + i\omega\mathbf{C} - \omega^2\mathbf{M}) U(\omega) = -\mathbf{M}\Lambda \ddot{U}_b(\omega) = \omega^2\mathbf{M}\Lambda U_b(\omega) \quad (82)$$

As usual, time domain response will be therefore obtained through Frequency Domain Analysis [4] making use of the Fast Fourier Transform. This reference simplified model was implemented in an independent matlab<sup>©</sup> code.

## 4.2 Reference Configuration

The reference configuration adopted for this study is the widely used 5MW NREL reference turbine. More precisely, the base configuration is the one defined for the OC3 (Offshore Code Comparison Collaboration) for the offshore 5MW NREL reference turbine on a monopile. Specific data can be found in Jonkman and Musial [7]. The main data for tower and substructure can be found in tables 1 and 2.

## 4.3 Verification cases

Table 3 lists the main characteristics of the input motions used for the four simplified verification cases presented herein together with the base configuration (fixed or compliant) in each case.  $\xi_t$  denotes the structural tower damping ratio. On the other hand, table 4 presents the parameters obtained for the SLPM from fitting the impedance functions corresponding to the foundation of this turbine [7]. The impedance functions were obtained from detailed boundary elements model [8].

## 4.4 Verification results

This section presents the validation results described in the previous section. Figure 4 present the comparisons between the results obtained using the modified version of OpenFAST and those of the reference inverted pendulum matlab code. Motions at the top of the tower, and at the platform are represented. It is shown that the agreement is very good in terms of displacements. It is worth highlighting, however, the major difference between both codes, being the OpenFAST model much more elaborated than

Parameter	Value
Tower-top height above mean sea level (MSL)	87.6 m
Tower base height above mean sea level	10.0 m
Water depth (from mean sea level)	20.0 m
Tower lenght	77.6 m
Water depth (from mean sea level)	20.0 m
Diameter at the base of the tower	6.0 m
Diameter at the top of the tower	3.87 m
Thickness at the base of the tower	0.027
Thickness at the top of the tower	0.019
RNA mass	349389.842 kg
RNA center of mass above tower top	1.96699 m
Second moment of inertia around RNA's center of mass	$I_{xx} = 4.37 \cdot 10^7 \text{ kg} \cdot \text{m}$
	$I_{yy} = 2.35 \cdot 10^7 \text{ kg} \cdot \text{m}$
	$I_{zz} = 2.54 \cdot 10^7 \text{ kg} \cdot \text{m}$

Table 1. Tower and turbine main properties, 5MW.

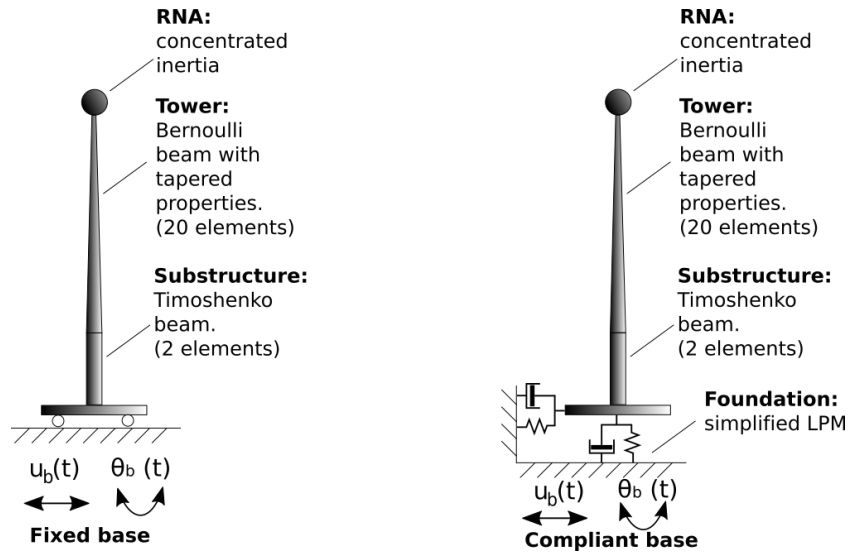


Figure 3. Depiction of the reference simple model used for comparison

Parameter	Value
Height	30.0 m
Diameter	6.0 m
Thickness	0.60 m

Table 2. Monopile main propeties

N	Motion	Base configuration	$\xi_t$	Input base motion
1	Lateral	Fixed base	5%	Quarter of sine ( $f = 0.1$ Hz, $A = 0.1$ m)
2	Rotational	Fixed base	2%	Quarter of sine ( $f = 0.1$ Hz, $A = 0.05$ m)
3	Lateral	Fixed base	2%	Chi-Chi earthquake
4	Lateral	Compliant base	2%	Chi-Chi earthquake

**Table 3.** Verification cases

$K_{\text{SLPM}}$	Value	$C_{\text{SLPM}}$	Value	$M_{\text{SLPM}}$	Value
$k_h$	5.478e+4	$c_h$	1.212e+7	$m_h$	55.92
$k_r$	1.078e+11	$c_r$	3.633e+8	$I_r$	1.0
$k_t$	2.274e+9	$c_t$	4.966e+7	$m_t$	5.047e+05
$k_z$	4.787e+9	$c_z$	2.117e+8	$m_z$	1.0
$k_{\text{tor}}$	7.13e+10	$c_{\text{tor}}$	4.414e+8	$I_{\text{tor}}$	8.60e+6
$h_1$	-4.794	$h_2$	-4.417	$h_3$	0.08194

**Table 4.** SLPM parameters

the reference model, and being the first one solved in time domain and the second one in frequency domain. As expected, response on a softer foundation (previously verified against the matlab reference model) provides a longer period. It also allows to see that the great influence that the properties of the foundation exert on the system global response. Table 5 shows the fundamental frequencies as a function of the assumed base condition.

Base condition	Fundamental frequency
Fixed base, fore-aft:	0.2797 Hz (T=3.58 s)
Compliant base, fore-aft:	0.2597 Hz (T=3.85 s)

**Table 5.** Fundamental frequencies obtained for Fixed Base and Compliant base conditions

## 5 ILLUSTRATION EXAMPLE

After having verified the implementation of the kinematic input motions for a simplified inverted pendulum configuration, this section illustrates the use of the code for the analysis of the seismic response of the offshore wind turbine while the turbine is operating and is subjected to wind, waves and currents. The NREL 5 MW reference OWT described above is considered here too. The simplified Lumped Parameter Model is used to represent the flexibility of the soil-foundation system (see Figure 5), as stated above. At the same time, the system is assumed to be subjected to vertically-incident shear waves. The Chi-Chi earthquake is considered as free-field ground-surface seismic action. The simulation is allowed to run for 220 seconds before the earthquake shaking arrive, in order to allow the dissipation of the transient response generated at the beginning of the simulation. No emergency shutdown is considered. The time-harmonic kinematic interaction factors corresponding to the monopile foundation were computed through the

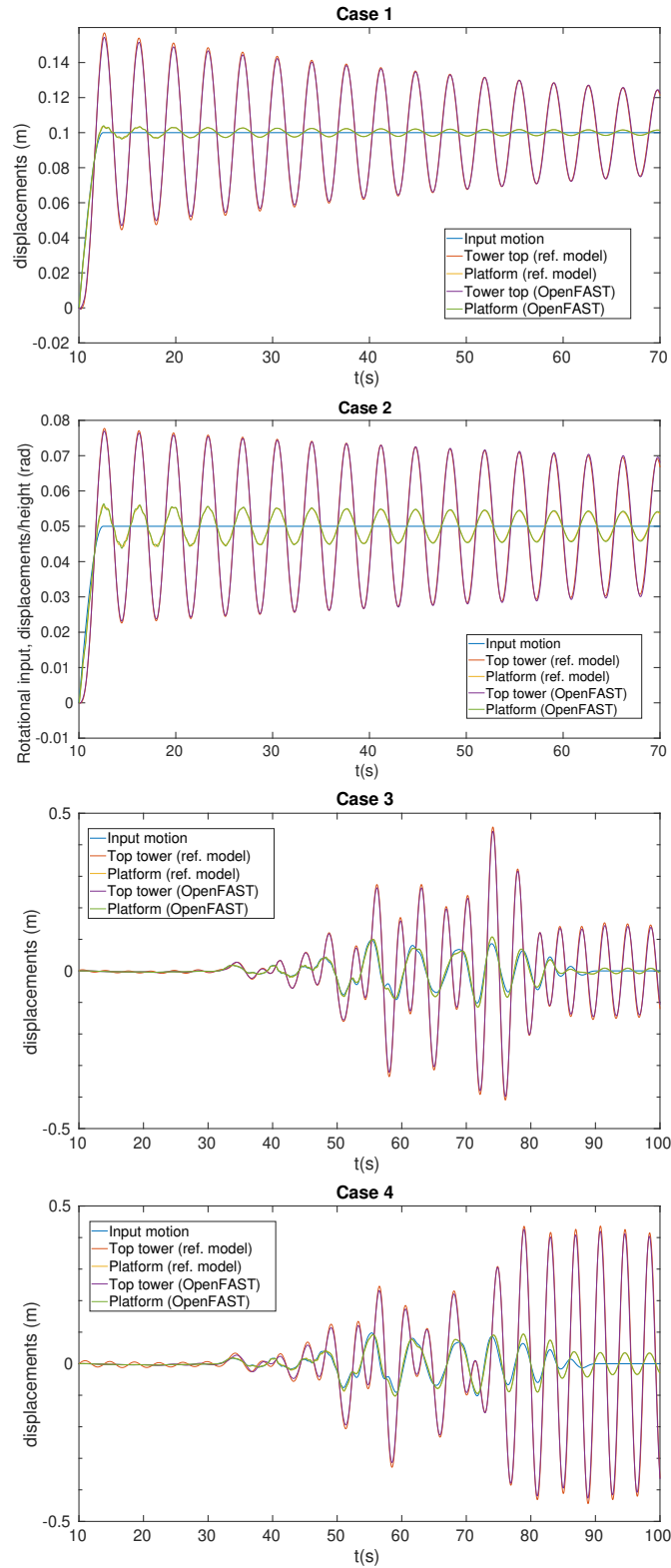
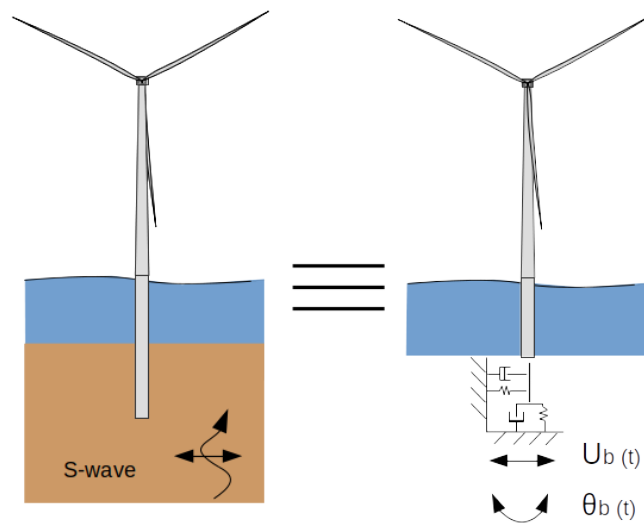


Figure 4. Results corresponding to verification cases

same boundary element model employed to compute the impedance functions [8]. These kinematic interaction factors allow to compute the translational and rotational kinematic input motions (see Figure 6) that are then defined at the base of the SLP.

Figure 7 presents the computed seismic response in terms of tower top displacements, tower top accelerations and mudline shear forces and bending moments in the monopile. Each plot presents the response of the OWT computed under four different loading situations: a) only environmental loads (wind, waves and currents); b) taking into account both translational and rotational foundation input motions; c) taking into account only translational foundation input motion (with zero rotational input motion); and d) considering the original seismic input motion as translational input motion, i.e., without taking into account the filtering produced by the pipe pile foundation.



**Figure 5.** Illustration example model

As expected, the seismic action increases the response of the structure in terms of displacements and accelerations at the tower top. Accelerations, in particular, increase by a factor of 3 due to the arrival of the earthquake. Bending moments and shear forces at mudline, on the contrary, are less affected by the earthquake, being the environmental loads the ones that contribute more importantly to the resulting internal efforts. The rotational component of the FIM produces an increase in the seismic response, as observed from the comparison of the responses computed taking or not into account the rotational input motion (red and green curves). However, this increase is not very significant when compared to the oscillations of the response of the system under the rest of loads. Finally, the difference between considering the original earthquake signal or the filtered earthquake signal is negligible.

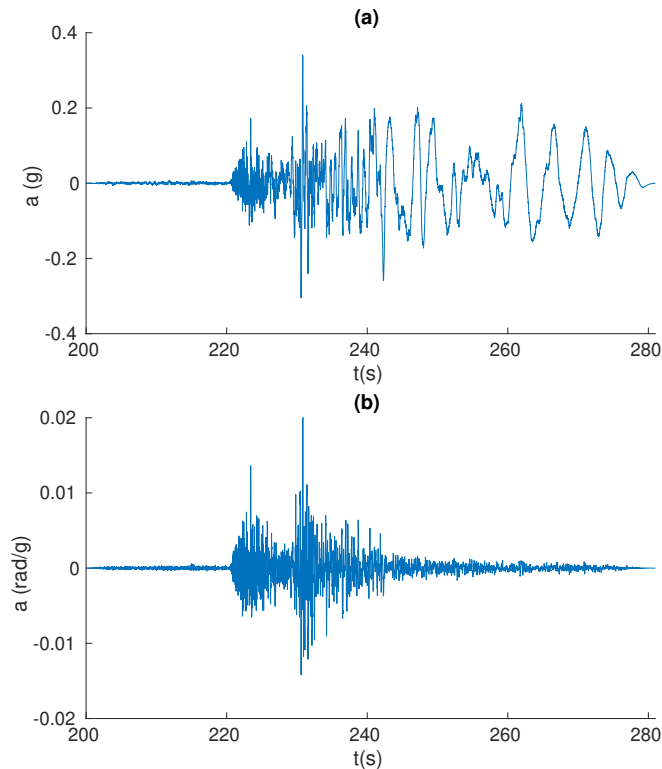


Figure 6. Lateral FIM (a) and Rotational FIM (b). Obtained from KIF of monopile foundation and Chi-Chi Earthquake

## 6 CONCLUSIONS

The paper develops the formulation needed for the implementation of seismic input motions and new dynamic soil-structure interaction capabilities into the open-source software OpenFAST, with the aim of facilitating the use of this tool for the seismic analysis of wind turbines.

Not only horizontal, but also vertical and rotational foundation input motions are considered. In the illustration example, horizontal and rotational foundation input motions are computed taking the monopile kinematic interaction factors into account, and the relevance of this filtering is also discussed.

On the other hand, the use of lumped parameter models is considered here as a tool to introduce soil-structure interaction into the model because this approach allows to take into account, not only the static stiffness of the foundation, but an approximation to its impedance, i.e., the dynamic stiffness and damping functions.

These capabilities have been implemented in OpenFAST, version 2.2.0, and the code can be downloaded here: [https://github.com/CarlosRomeroSanchez/openfast\\_2.2.0\\_seismic](https://github.com/CarlosRomeroSanchez/openfast_2.2.0_seismic). The authors are now working on the generalization of the formulation to non-uniform input motions, and its implementation in the latest version of OpenFAST.

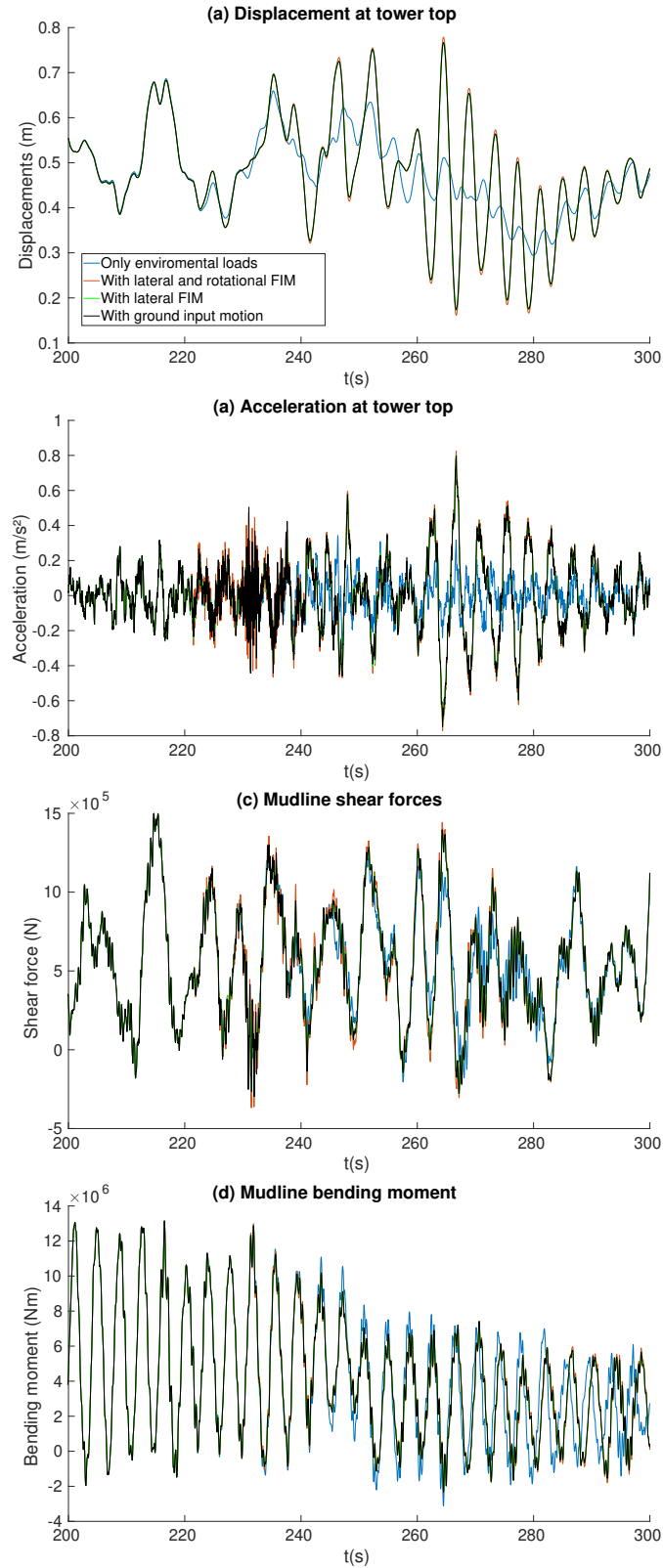


**Figure 7.** Results corresponding to illustration example

## ACKNOWLEDGEMENTS

This research was funded by Consejería de Economía, Conocimiento y Empleo (Agencia Canaria de la Investigación, Innovación y Sociedad de la Información) of the Gobierno de Canarias and FEDER through research project ProID2020010025.

## REFERENCES

- [1] EWEA, Offshore Wind in Europe - Key trends and statistics 2020, *Wind Europe*, (2021).
- [2] OpenFAST Documentation, Release v3.1.0, National Renewable Energy Laboratory, (2022). <https://openfast.readthedocs.io/en/main/>. Code published at <https://github.com/OpenFAST/openfast>.
- [3] Damiani R., Jonkman J., Hayman G., *SubDyn user's guide and theory manual*, techreport NREL/TP-5000-63062, National Renewable Energy Laboratory, (2015).
- [4] Chopra A.K., *Dynamics of Structures. Theory and applications to earthquake engineering*. Pearson, 7th ed. edition, (2017).
- [5] Carbonari S., Morici M., Dezi F., Leoni G., *A lumped parameter model for time-domain inertial soil-structure interaction analysis of structures on pile foundations*, Earthquake Engineering & Structural Dynamics, Vol. 47, 2147-2171.(2018)
- [6] González F., Padrón L. A., Carbonari S., Morici M., Aznárez J. J., Dezi F., Leoni G., *Seismic response of bridge piers on pile groups for different soil damping models and lumped parameter representations of the foundation*. Earthquake Engineering & Structural Dynamics, Vol. 48, 306–327 (2019).
- [7] Jonkman J., Musial W., *Offshore Code Comparison Collaboration (OC3) for IEA Task 23 Offshore Wind Technology and Deployment*, techreport NREL/TP-5000-48191, National Renewable Energy Laboratory, (2010).
- [8] Bordón J. D. R., Aznárez J. J., Maeso O., *Dynamic model of open shell structures buried in poroelastic soils*, Computational Mechanics, Vol. 60, 269–288 (2017).